Effect of tooth profile modification on the durability of planetary hub gears

Ehsan Fatourehchi, Mahdi Mohammadpour, Paul D. King and Homer Rahnejat

Wolfson School of Mechanical Engineering,
Loughborough University,
LE113TU, England, UK
Email: Ehsan.fatourehchi@gmail.com
Email: M.Mohammad-Pour@lboro.ac.uk
Email: P.D.King@lboro.ac.uk
Email: H.Rahnejat@lboro.ac.uk
*Corresponding author

Gareth Trimmer

JCB Transmission,
Wrexham Industrial Estate,
Wrexham, UK
Email: gareth.trimmer@jcb.com

Abstract: Planetary systems offer the advantage of desired speed-torque variation with a lighter, compact and coaxial construction than the traditional gear trains. Frictional losses and noise, vibration and harshness (NVH) refinement are the main concerns. Modification of gear teeth geometry to reduce friction between the mating teeth flanks of vehicular planetary hubs, as well as refining NVH under varying load-speed conditions is one of the remedial actions. However, implementing modifications can result in reduced structural integrity and system durability. Therefore, a contradiction may arise between assuring a high degree of durability and achieving better transmission efficiency, which necessitates detailed system optimisation. An integrated multi-disciplinary analytical approach, including tribology and sub-surface stress analysis is developed. As a preliminary step, tooth contact analysis (TCA) is performed to obtain contact footprint shape of meshing gear teeth pairs, as well as contact kinematics and applied load distribution. Then, an analytical time-efficient elastohydrodynamic lubrication (EHL) analysis of elliptical point contact of crowned spur gear teeth is carried out to observe the effect of gear tip relief modification upon planetary hub sub-surface stresses.

Keywords: transmission system durability; gear tooth modification; planetary wheel hub systems.

Reference to this paper should be made as follows: Fatourehchi, E., Mohammadpour, M., King, P.D., Rahnejat, H. and Trimmer, G. (2019) 'Effect of tooth profile modification on the durability of planetary hub gears', *Int. J. Powertrains*, Vol. 8, No. 1, pp.40–57.

Biographical notes: Ehsan Fatourehchi is a Development Engineer at the Scania AB Company. He received his PhD from the Loughborough University. His PhD project was about the high-performance transmission systems efficiency, and the overall aim of his PhD was to develop a predictive modelling/analysis tool as an aid for thermal functioning of high-performance transmission systems operating under dry-sump lubrication system.

Mahdi Mohammadpour is a Senior Lecturer in Dynamic Research Group of the Wolfson School of Mechanical, Electrical and Manufacturing of Loughborough University. He received his PhD in Tribodynamics from the Loughborough University in 2014. His research focuses mainly on dynamics, tribology, energy efficiency and the related subjects. He is an Associate Editor for the *International Journal of Powertrains*. He is also on editorial board of *Shock and Vibration Journal*.

Paul D. King is a Senior Lecturer in Dynamics Research Group of the Wolfson School of Mechanical, Electrical and Manufacturing of Loughborough University. His research focuses mainly on tribology and vehicle dynamics.

Homer Rahnejat is the Chair of Dynamics and Head of Dynamic Research Group of the Wolfson School of Mechanical, Electrical and Manufacturing of Loughborough University. He received his PhD from the Imperial College in 1984. He is the Editor-in-Chief of *Proceedings of Institution of Mechanical Engineers*, *Part K: Journal of Multi-body Dynamics and MDPI's Lubricants*. He has been the Chairman, co-Chair and keynote speaker at many research conferences.

Gareth Trimmer is the Axle Engineering Manager for JCB. He is a graduate from the Cranfield University with 20 years post-graduate experience in axle design and development for the off-highway construction and agricultural sectors.

This paper is a revised and expanded version of a paper entitled 'Effect of tooth profile modification on the performance and durability of planetary hub gears' presented at International Conference on Advanced Vehicle Powertrains, Hangzhou, China, 25–27 September 2017.

1 Introduction

A large number of mechanical applications, ranging from wind turbines to automotive powertrains use planetary gears. This is because they provide a set of transmission ratios and provide improved efficiency relative to fixed axes transmissions (Talbot et al., 2012).

A number of studies have focused on the transmission efficiency of planetary gear systems (Talbot et al., 2012; Marques et al., 2015; Mohammadpour et al., 2016; Fatourehchi et al., 2018). However, in many cases improving the transmission efficiency can result in reduced structural integrity and system durability. This necessitates an in-depth stress analysis, integrated with analysis of system efficiency in order to arrive at an optimal practical solution.

Evaluation of sub-surface stress distribution in medium to highly loaded contacts is important as these determine the fatigue life of machine elements. Highly loaded gear contacts are generally subjected to high sub-surface stresses. Lundberg and Palmgren

(1949) carried out one of the first studies in this field. They investigated fatigue mechanism in roller bearings and showed the significance of generated sub-surface stress field. They discovered that one of the critical parameters in initiating fatigue cracks in a contact is the location of maximum sub-surface shear stress. The cyclic nature of contact stresses causes the crack to propagate and finally reach the contacting surface, leading to the formation of spalls. A comprehensive treatment of 3D sub-surface stress field for elastohydrodynamic contacts (such as gears and bearings) was reported in (Johns-Rahnejat and Gohar, 1997), which showed that the reversing cyclic orthogonal shear stresses play a more poignant role in load bearing conjunctions. In elastohydrodynamic contacts, the presence of the pressure spike in the vicinity of the contact outlet also sets up a localised sub-surface stress field with higher maximum shear stresses which occur closer to the contact surface as shown by Teodorescu et al. (2007) in the case of cam-tappet contact. This localised field can initiate premature spalling (Johns-Rahnejat and Gohar, 1997). Recently, Li et al. (2012) developed a numerical model to predict fatigue crack formation in spur gear contacts working under mixed elastohydrodynamic regime of lubrication. The model was compared with measured gear fatigue stress-life data, showing reasonable accuracy in predicting the crack nucleation fatigue life, as well as the location of the critical failure sites. Fatourehchi et al. (2016) developed a numerical model to investigate the effect of different gear teeth modifications on spur gear power loss and durability of high performance transmission systems. Nevertheless, both studies were associated with a single gear contact operating under moderate to high speeds.

With regard to planetary gears, Jao et al. (2006) performed a fatigue test on an automatic transmission planetary gear which consisted of a forward sun gear, a reverse sun gear, three short and three long pinions. They observed that macro-pitting and bending fatigue are the primary causes of failure in gears. Dong et al. (2013) developed a simplified model to predict the fatigue life of contacting gears of a wind turbine planetary gear sets operating under dynamic conditions. Their study showed that pitting is more likely to occur on the sun gear rather than the planet gears. Moreover, the recess area is the critical location in terms of pitting. This is because the equivalent contact radius within the recess area of the sun and planet gears is much smaller than at the pitch and contacting regions. Therefore, maximum contact pressure occurs in the recess area.

Bahk and Parker (2013) developed an analytical model to investigate the effect of tooth profile modification on spur planetary gear vibration. Tooth profile modification can minimise vibration in certain vibration modes than others. Therefore, the most active modes need to be considered when applying optimal gear tooth profile modification in order to minimise gear vibration.

Inevitable manufacturing errors cause the applied load not to be shared equally within the different sun-planet and planet-ring meshes. This is another parameter which can be troublesome for gear durability. Ligata et al. (2008) carried out an experimental study of the effects of manufacturing errors on planetary system gear stresses. They studied the influence of the number of planets, torque levels, and the carrier pinhole positional errors. Their results indicated that increasing the number of planets makes the generated stresses more sensitive to the carrier pinhole positional error. Fatourehchi et al. (2017) developed a tribo-dynamic model to investigate the effect of mesh phasing due to manufacturing errors on the planetary system efficiency and noise, vibration and harshness (NVH) refinement. The model was capable of predicting the optimal level of combined efficiency and NVH performance of a planetary system.

In this paper, a parametric analysis is conducted in order to investigate the effect of different extents of tooth profile modifications on planetary hub gears' sub-surface stresses in off-highway applications. There has been a dearth of work reported for this type of planetary hub gears for trucks and off-highway vehicles operating under high loads and low speeds. These operational conditions are critical in terms of tribology with increased contact pressures of up to 1.2 GPa and a sub-micrometre lubricant film thickness. Planetary hub systems are particularly compact, resulting in teeth pair contacts of highly concentrated nature. Fatigue spalling due to sub-surface stress field is common in practice. Thus, a numerical model capable of predicting the parameters which affect planetary hub gears' generated sub-surface stresses is the key to achieving a reliable system. The developed model provides realistic conditions with rapid cost-effective simulations. It takes into account the shear in the contacting region, as well as the normal generated pressures for better estimation of the sub-surface stress field. This approach has not hitherto been reported in literature for planetary wheel hub gears.

2 Planetary hub configuration

The studied planetary hub gear system is shown schematically in Figure 1. Figure 1 also shows the power flow from the gearbox through to the planetary wheel hubs. The transmission ratio, speed and torques at different transmission stages are also indicated in Figure 1. The sun gear is attached to the input shaft which transfers power from the differential. The ring gear is attached and fixed to the housing. The carrier transfers the output power of the planetary hub system to the wheels. The planetary system comprises three planet gears. The study assumes no misalignment in the system. It is also assumed that the input power from the sun gear is divided equally among the planets.

Figure 1 Schematic representation of the planetary wheel hub gears configuration and the power flow

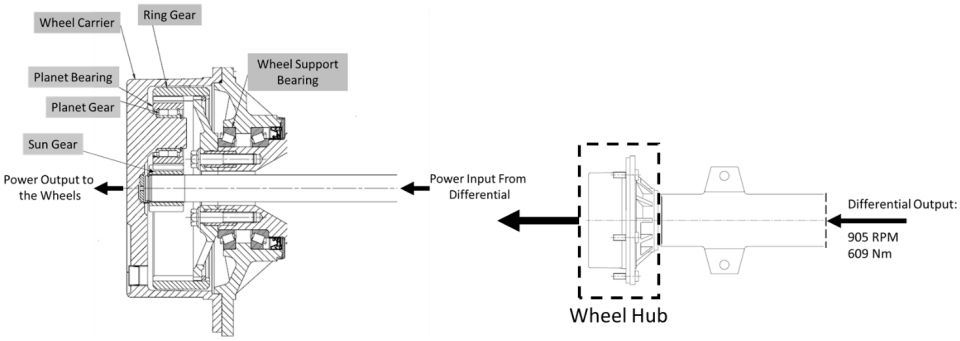

3 Methodology

Normal generated contact pressure and tangential traction distributions over the contact patch at any location along a meshing cycle are needed in order to evaluate the generated sub-surface stress field. An integrated tooth contact analysis (TCA) and an analytical

elastohydrodynamic method are introduced. At any location along the meshing cycle, the instantaneous radii of curvature of the meshing teeth, as well as contact surface velocities and the orthogonal meshing contact loads are obtained through the TCA. These parameters form the input to the analytical elastohydrodynamic analysis, yielding the normal generated pressures (assumed as Hertzian) and viscous friction (i.e., tangential traction). The methodology is based on quasi-static analysis. This is necessary to perform rapid cost-effective simulations, suitable for industrial use. Therefore, dynamics of the planetary hub system is neglected. Furthermore, this study does not take into account the effect of manufacturing errors on the planetary system durability.

3.1 Tooth contact analysis

The approach of Vijayakar (2000) and Xu and Kahraman (2007) is utilised to develop the TCA model. The developed model obtains the instantaneous contact geometry, rolling/sliding velocity and load share per teeth pair contact (Xu and Kahraman, 2007; Karagiannis et al., 2012) for simultaneous meshing of sun-planet and planet-ring contacts in the planetary hub system.

3.2 Subsurface stresses

Contacting gear surfaces transmit the generated normal pressures and tangential traction due to viscous friction. Normal pressure $p(x)$ and tangential traction $q(x)$ over the strip ($-b < x < a$) in an elastic half-space are shown in Figure 2.

According to Johnson (1985), the sub-surface stress distribution at an arbitrary point A (Figure 2) within the body of contacting solids induced by $p(x)$ and $q(x)$ becomes:

$$\sigma_x = -\frac{2z}{\pi}\int_{-b}^{a}\frac{p(s)(x-s)^2\,ds}{\left[(x-s)^2+z^2\right]^2} - \frac{2z^2}{\pi}\int_{-b}^{a}\frac{q(s)(x-s)^3\,ds}{\left[(x-s)^2+z^2\right]^2} \tag{1}$$

$$\sigma_z = \frac{2zh3}{\pi}\int_{-b}^{a}\frac{p(s)ds}{\left[(x-s)^2+z^2\right]^2} - \frac{2z^2}{\pi}\int_{-b}^{a}\frac{q(s)(x-s)ds}{\left[(x-s)^2+z^2\right]^2} \tag{2}$$

$$\tau_{xz} = -\frac{2z^2}{\pi}\int_{-b}^{a}\frac{p(s)(x-s)ds}{\left[(x-s)^2+z^2\right]^2} - \frac{2z}{\pi}\int_{-b}^{a}\frac{q(s)(x-s)^2\,ds}{\left[(x-s)^2+z^2\right]^2} \tag{3}$$

The elastohydrodynamic model is developed to obtain the tangential traction due to viscous friction, $q(x)$. The proposed analytical model is time-efficient, simulating a meshing cycle of a spur gear pair in a couple of seconds. This is essential in performing a parametric study of the effect of gear tip relief modification upon planetary hub generated sub-surface stress field. The contact pressure is obtained based on Hertzian theory (which closely agrees with the prevailing elastohydrdynamic conditions, particularly for the usually starved transmission gearing). Therefore, the usually generated elastohydrodynamic lubrication (EHL) pressure spike at the vicinity of the contact outlet is neglected. The method is explained in the next section.

Figure 2 Normal pressure and tangential traction distribution over the solid surface [after Johnson (1985)]

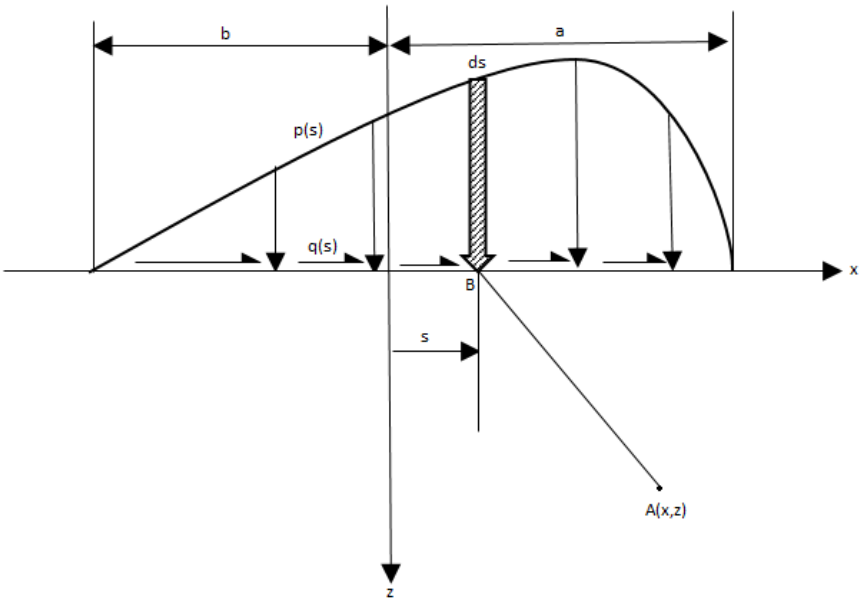

According to the Hertzian theory:

$$p(x) = \frac{2W}{\pi_{a^2}}(a^2 - x^2)^{1/2} \tag{4}$$

where:

$$a^2 = \frac{4WR}{\pi E_r} \tag{5}$$

The maximum pressure is:

$$p_0 = \left(\frac{WE_r}{\pi R}\right)^{1/2} \tag{6}$$

The key points with regard to the structural integrity of the mating gear teeth surfaces is the choice of yielding criterion for inelastic deformation. The general consensus for bearing and gear surfaces is the cyclic repetitive nature of orthogonal shear stresses, given by equation (3). These occur in depths closer to the contacting surface with a larger double amplitude (cyclic tensile-compressive). The cyclic nature of gear contact causes the bulk material to be sheared in one direction and then in the opposite sense. The alternating shear stress field, τ_{zx} occur in pairs at 90° to each other in the auxiliary planes (Johns-Rahnejat and Gohar, 1997). The equivalent stress, σ_e with the alternating shear stress hypothesis is (Johns-Rahnejat, 1988):

$$\sigma_e = 2|\tau_{zxmaz}| \tag{7}$$

where the double amplitude for σ_e remains approximately the same with any additional surface traction (Gohar and Rahnejat, 2008). The onset of yielding according to the alternating shear stress hypothesis is when the equivalent stress reaches half the yield stress of the material (i.e., structural integrity is assured, when: $\sigma_e < 1/2\ \sigma_y$).

3.3 The elastohydrodynamic model

High contact pressures of up to 1.2 GPa, in the planetary wheel hub system of trucks and off-highway applications can result in high pressure viscous shear in the contact. Mixed regime of lubrication is also expected due to very thin lubricant films. Tangential traction in the contact is obtained as:

$$q = \frac{(f_v + f_b)}{A} \tag{8}$$

where f_v is the viscous friction and f_b is the boundary friction in the contact, and A is the apparent contact area.

3.3.1 Viscous friction

Evans and Johnson (1986) developed an analytical method to determine viscous friction in elastohydrodynamic contacts, where the coefficient of friction is obtained as:

$$\mu = \frac{f_v}{W} = 0.87\alpha\tau_0 + 1.74\frac{\tau_0}{p}\ln\left[\frac{1.2}{\tau_0 h_{c0}}\left(\frac{2K^*\eta_0}{1+9.6\xi}\right)^{\frac{1}{2}}\right] \tag{9}$$

where W is the normal contact load, obtained from the TCA model, and ξ is:

$$\xi = \frac{4}{\pi}\frac{K}{h_{c0}/R}\left(\frac{\overline{p}}{E'RK'\rho'c'U_r}\right)^{1/2} \tag{10}$$

Chittenden et al.'s (1985) equation is used to calculate the thin lubricant film thickness under the instantaneous operating conditions which is required for equation (10).

$$h^*_{c0} = 4.31U_e^{0.68}G_e^{0.49}W_e^{-0.073}\left\{1-\exp\left[-1.23\left(\frac{R_y}{R_x}\right)^{2/3}\right]\right\} \tag{11}$$

where the dimensionless groups are expressed as:

$$U_e = \frac{\pi\eta_0 U}{4E_r R_x},\ W_e = \frac{\pi W}{2E_r R_x^2},\ G_e = \frac{2}{\pi}(E_r\alpha),\ h^*_{c0} = \frac{h_0}{R_x}$$

Table 1 lists the lubricant properties.

Table 1 Lubricant properties

Pressure viscosity coefficient (Pa^{-1})	2.38×10^{-8}
Lubricant Atmospheric dynamic viscosity at 100°C (Pa.s)	0.0144
Ambient value of lubricant limiting shear stress (MPa)	2
Thermal conductivity of fluid (W/mK)	0.140
Pressure-induced shear coefficient (ε)	0.047

3.3.2 Boundary friction

The high contact pressures of planetary gear systems result in thin lubricant films of the order of surface roughness. Therefore, some degree of interaction of asperities on the counter face contacting surfaces occurs. These interactions promote boundary friction. In this study, Greenwood and Tripp (1970) method is utilised in predicting boundary friction. When the Stribeck's oil film parameter falls within the range: $1 < \lambda = \frac{h_{c0}}{\sigma} < 2.5$, mixed regime of lubrication occurs. Under these conditions, the share of contact load which is carried by the contact of asperity heights is:

$$W_a = \frac{16\sqrt{2}}{15}\pi(\xi\beta\sigma)^2\sqrt{\frac{\sigma}{\beta}}E'AF_{5/2}(\lambda) \tag{12}$$

where the statistical function $F_{5/2}(\lambda)$, assuming a Gaussian distribution of asperities is obtained as (Teodorescu et al., 2005):

$$F_{5/2} = \begin{cases} -0.004\lambda^5 + 0.057\lambda^4 - 0.29\lambda^3 + 0.784\lambda^2 - 0.784\lambda + 0.617 & \text{for } \lambda < 2.5 \\ 0; & \text{for } \lambda \geq 2.5 \end{cases} \tag{13}$$

The roughness parameter ($\xi\beta\sigma$) for steel surfaces is generally in the range 0.03–0.07 (Greenwood and Tripp, 1970). Average asperity slope (Gohar and Rahnejat, 2008), σ/β, is usually in the range of 10^{-4}–$10^{-2.}$ In the current study, these parameters were obtained through measurement of a typical gear tooth topography as: $\xi\beta\sigma = 0.055$ and $\sigma/\beta = 10^{-3}$ (Mohammadpour et al., 2014).

A thin film of boundary active lubricant additives (a tribo-film) is usually adsorbed or bonded to the summit of the contacting asperities or is entrapped in their inter-spatial valleys. This lubricant film is subjected to non-Newtonian shear, thus:

$$f_b = \tau_L A_a \tag{14}$$

where τ_L is the lubricant's limiting shear stress:

$$\tau_L = \tau_0 + \varepsilon^* P_m \tag{15}$$

where the mean pressure P_m is obtained as:

$$P_m = \frac{W_a}{A_a} \tag{16}$$

The asperity contact area is (Greenwood and Tripp, 1970):

$$A_a = \pi^2(\xi\beta\sigma)AF_2(\lambda) \tag{17}$$

The statistical function $F_2(\lambda)$ is obtained as (Teodorescu et al., 2005; Mohammadpour et al., 2014):

$$F_2(\lambda) = \begin{cases} -0.002\lambda^5 + 0.028\lambda^4 - 0.173\lambda^3 + 0.526\lambda^2 - 0.804\lambda + 0.500 & \text{for } \lambda < 2.5 \\ 0; & \text{for } \lambda \geq 2.5 \end{cases} \tag{18}$$

4 Results and discussion

High impact loads and sharp rises in the contact pressures are more likely to occur for gear pairs with no tip relief. Under these conditions, gear teeth tip relief through removal of material ensures smoother gradual changes in profile. Applying tip relief in involute teeth can also relieve impact loads as teeth pairs come into contact. To achieve the optimum tip relief, its extent in length and amount should be determined. Figure 3 is a schematic representation of tip relief modification, showing both its amount and length.

The planetary wheel hub gears of the JCB Max-Trac rear differential is investigated here. The input torque to the sun gear from the differential is 609 Nm at the speed of 906 rpm. The gear data are listed in Table 2.

Figure 3 Schematic representation of tip relief modification

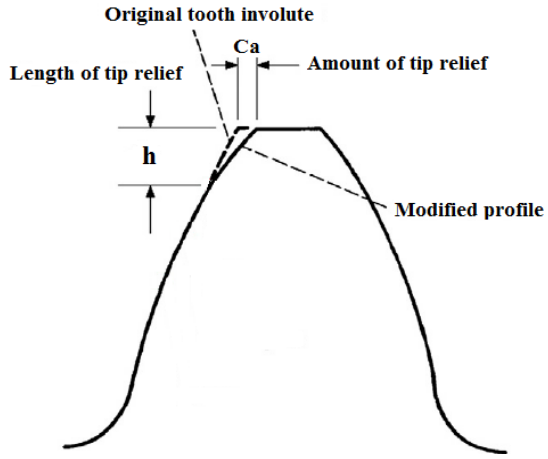

Table 2 The gearbox data

Radius of sun gear	26 mm
Radius of planet gear	43 mm
Radius of ring gear	115 mm
Number of teeth for sun gear	15
Number of teeth for planet gear	25
Number of teeth for ring gear	66
Pressure angle	20°
Helix angle	0°

Two parameters are involved in the tip relief modification. These are the amount of tip relief and the length of the relieved region. Firstly, the effect of gear teeth tip relief amount is considered. Secondly, the influence of gear teeth tip relief length is investigated.

It should be noted that the results are plotted against the angular position along the path of meshing contact progression. The effect of variation of tip relief amount and tip relief length on the length of line of action is negligible and therefore, different characteristics of contact are plotted against the non-dimensional 'position along the meshing cycle'. It varies between 0 to 1, where '0' refers to the angular position at the onset of meshing and '1' refers to angular position at the end of a meshing cycle.

4.1 Effects of tip relief amount

The amount of tip relief (specified as C_a in Figure 3) is changed from 25% to 150% of the current baseline design in order to investigate the effect of tip relief amount on the generated sub-surface stresses. Tip amounts of relief for different scenarios are listed in Table 3.

Table 3 Amount of tip relief for different scenarios

Scenario	*Tip relief amount [%]*		
	Sun	*Planet*	*Ring*
1	150	150	150
2	125	125	125
3 (current design)	100	100	100
4	75	75	75
5	50	50	50
6	25	25	25

Figure 4 shows the effect of change in tip relief amount on the contact parameters (i.e., radii of curvature, rolling velocity and normal load) for a meshing cycle for both the sun-planet and the planet-ring contacts.

Figure 4 shows that increasing the amount of tip relief increase the shift in the radii of curvature and the rolling/sliding velocity at the affected region. The sudden shift is due to the use of actual coordinate information created by a simulation of the cutting process which is embedded in the utilised TCA model (Vijayakar, 1996). Moreover, this increases the duration of single contact over a meshing cycle.

According to the alternating shear stress hypothesis (Johns-Rahnejat and Gohar, 1997; Johns-Rahnejat, 1988), Figures 5 and 6 illustrate the variation of maximum double shear stress magnitude along the meshing cycle for different applied tip relieves for the planet-ring and the sun-planet contacts respectively.

Figure 4 Contact parameters for sun-planet and planet-ring contacts along the meshing cycle for different tip relief amounts

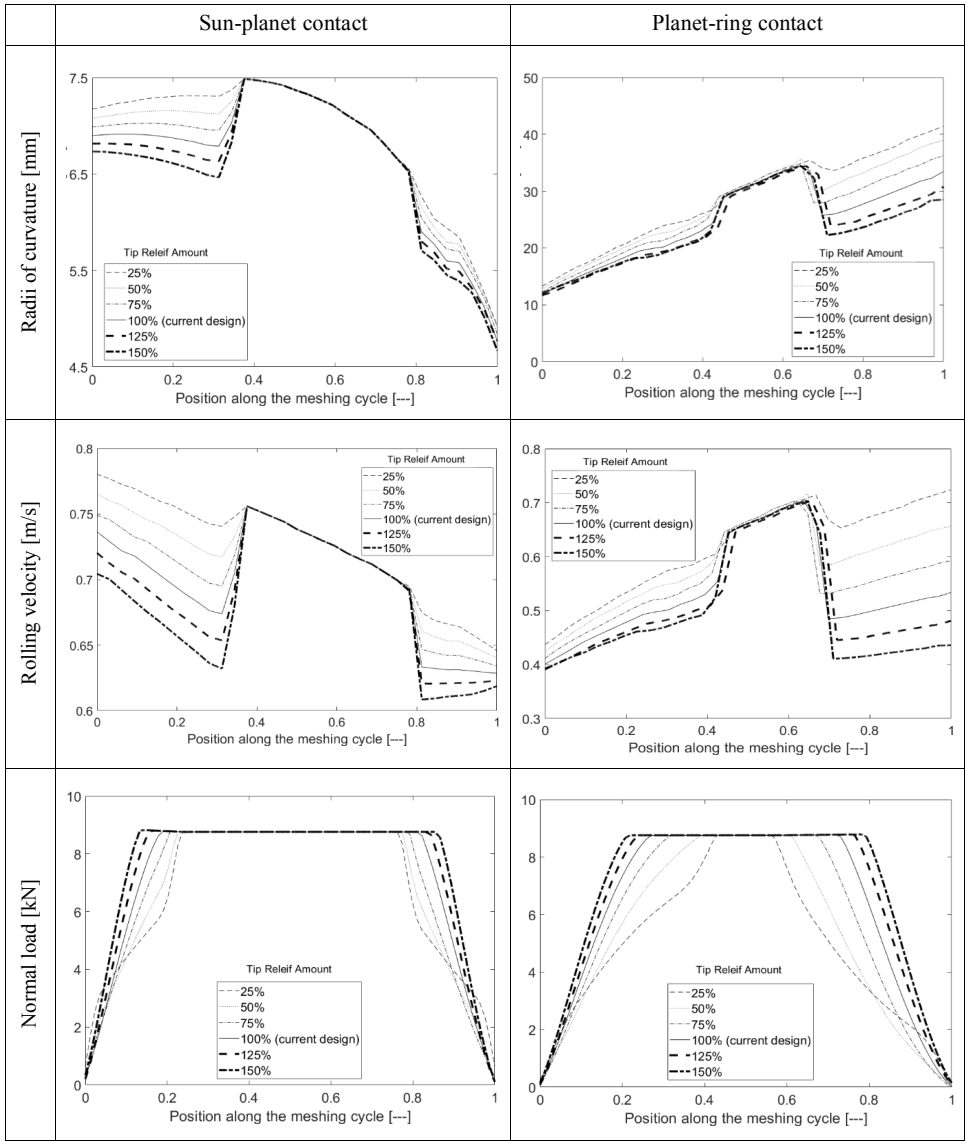

Figure 5 Double amplitude reversing orthogonal shear stress along the meshing cycle for different amounts of tip relief; planet-ring contact

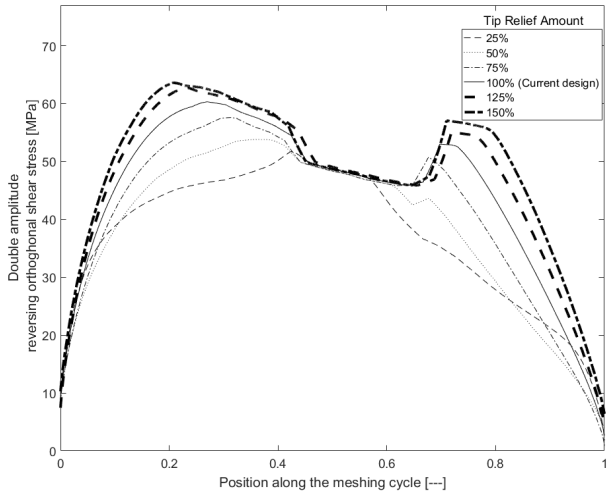

Figure 6 Double amplitude reversing orthogonal shear stress along the meshing cycle for different amounts of tip relief; sun-planet contact

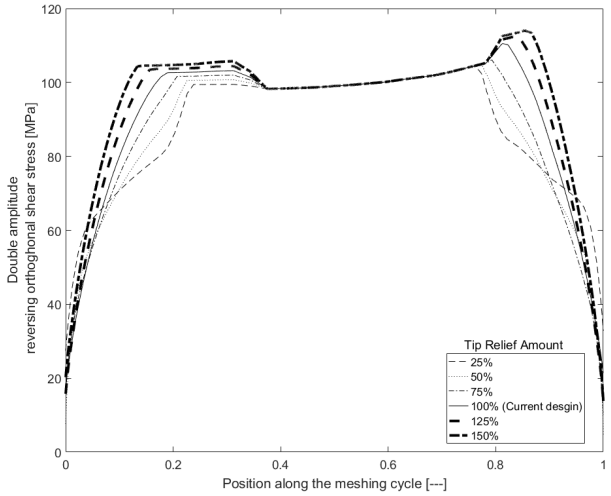

The tooth's hardened steel yield stress is 470 MPa. Therefore, based on the shear stress criterion described in Section 3.2, the double amplitude of the alternating shear stress (i.e., the equivalent stress) should not exceed 235 MPa. According to Figures 5 and 6, the equivalent stress remains below this limit for both planet-ring and sun-planet contacts. Increasing the amount of tip relief, the effect of alternating shear stresses becomes more pronounced. One should note that in this study, only the sub-surface shear stress field is considered as the measure for durability. Therefore, other durability parameters such as scuffing and scratching as well as NVH refinement and efficiency should also be taken into account.

Furthermore, the maximum amount of the equivalent stress in sun-planet contact is almost 50 MPa higher than that for the planet-ring contact, which indicates the fatigue failure is more likely to occur in the sun-planet contact which is in agreement with the findings in (Jao et al., 2006).

4.2 Effect of tip relief length

In order to investigate the effect of tip relief length (specified as *h* in Figure 3) on induced sub-surface stresses, the relief length is reduced from the current design (baseline value) by up to 35%. Table 4 shows the changes in the tip relief length for different scenarios.

Figure 7 shows the effect of change in the tip relief length on the contact parameters (i.e., radii of curvature, rolling velocity and normal load) for a meshing cycle for both the sun-planet and the planet-ring contacts.

Table 4 Length of tip relief for different scenarios

Scenario	*Length of tip relief [%]*		
	Sun	*Planet*	*Ring*
1 (current design)	100	100	100
2	75	75	75
3	50	50	50
4	37.5	37.5	37.5
5	35	35	35

Figure 7 shows that changes in the tip relief length, slightly decrease the radii of curvature and rolling velocity at the affected region in cases with over 50% change. Decreasing the length of tip relief by lower amounts (i.e., studied cases of 37.5% and 35%) causes a sudden change in the radii of curvature and the corresponding contact rolling velocity. Increasing the tip relief length slightly increases the duration of a single contact over a meshing cycle, where it is more pronounced in the case of planet-ring gear contact.

Using the alternating shear stress hypothesis (Johns-Rahnejat and Gohar, 1997; Johns-Rahnejat, 1988), Figures 8 and 9 illustrate the variation of double amplitude reversing orthogonal shear stress along the meshing cycle for different applied tip relief lengths for the planet-ring and sun-planet contacts respectively.

The results in Figures 8 and 9 show that the equivalent stress remains below the critical limit of 235 MPa for both the planet-ring and the sun-planet contacts. By

increasing the tip relief length, the effect of alternating shear stresses becomes more pronounced. These results suggest that the baseline design has the potential of improvement from a durability view-point. Again, it should be noted that the limiting sub-surface stress levels should be used in a trade-off with the efficiency and other performance measures such as the root stresses and scuffing-scratching as well as NVH refinement.

Figure 7 Contact parameters for sun-planet and planet-ring contacts along the meshing cycle for different tip relief lengths

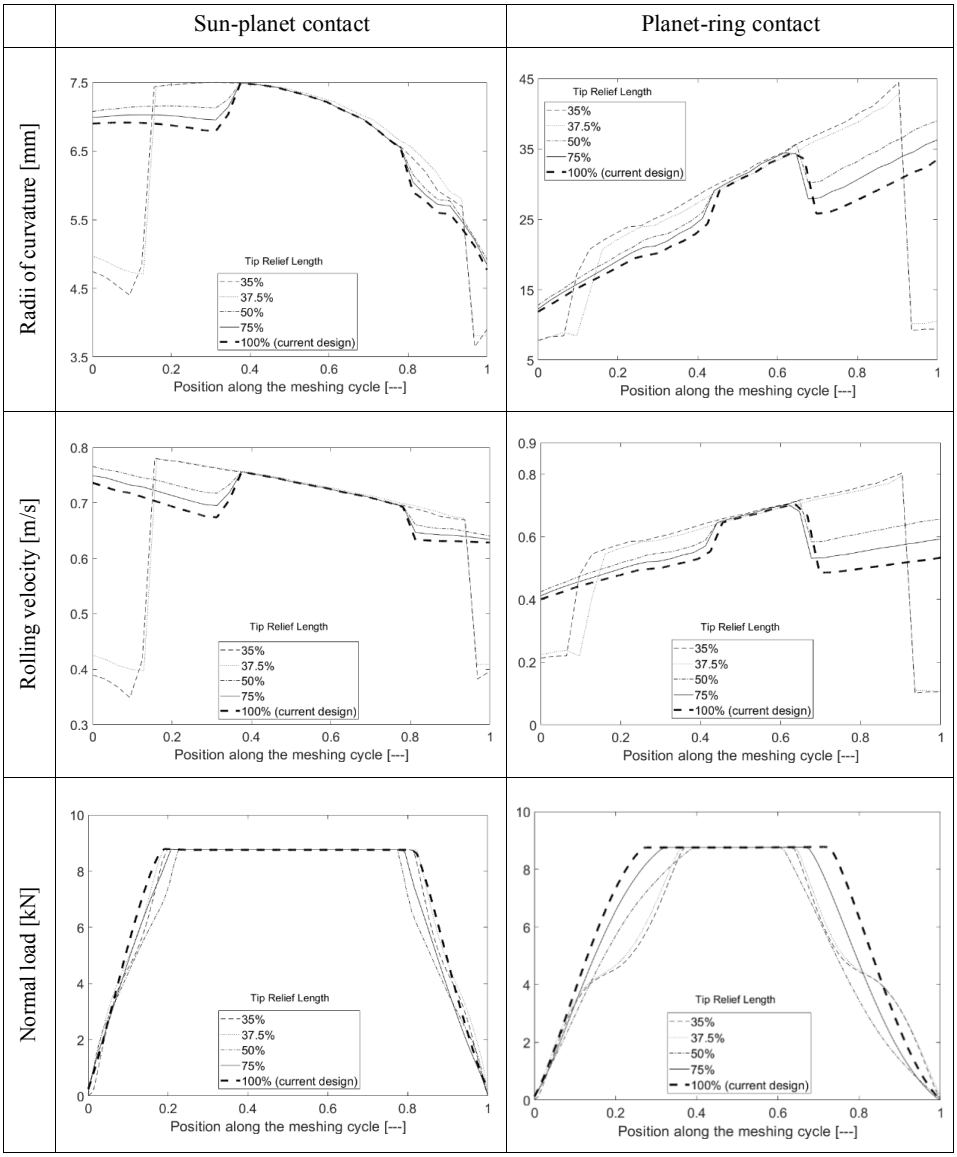

Figure 8 Double amplitude reversing orthogonal shear stress along the meshing cycle for different tip relief length; planet-ring contact

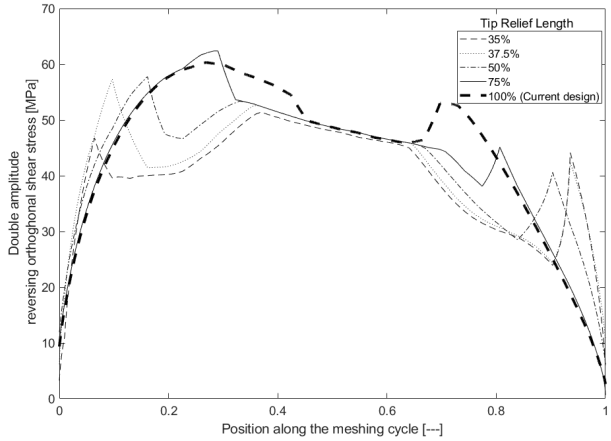

Figure 9 Double amplitude reversing orthogonal shear stress along the meshing cycle for different amounts of tip relief length; sun-planet contact

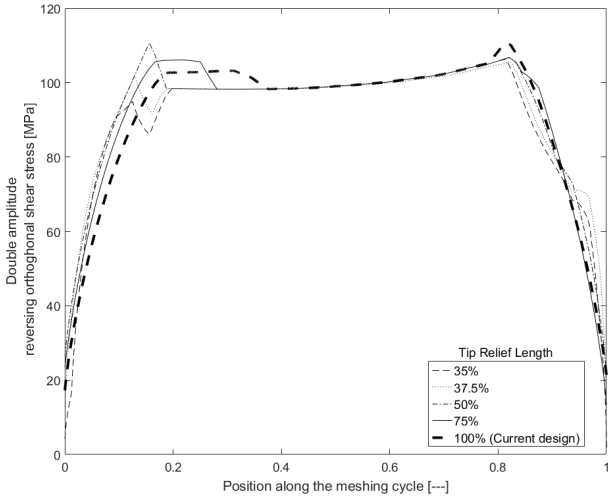

5 Conclusions

The study investigates the effect of tip relief (length and amount) modifications on the durability of planetary wheel hub gears of off-highway vehicles.

The following conclusions are made:

1 In general, the generated contact pressures are higher in sun-planet contact. Therefore, the maximum equivalent stress in the sun-planet contact is higher than that for the planet-ring contact.

2 In terms of tip relief modification, increasing both the amount of tip relief and its length leads to an increase in sub-surface shear stresses in mid-meshing cycle. Applying tip relief increases the duration of single contact time along the meshing cycle with the highest applied load and generated contact pressure.

3 By increasing the tip relief length, the effect of alternating shear stresses becomes more pronounced.

4 The presented sub-surface stress field should be in a trade-off with other performance and structural integrity measures such as root stresses, as well as transmission efficiency and NVH.

References

Bahk, C.J. and Parker, R.G. (2013) 'Analytical investigation of tooth profile modification effects on planetary gear dynamics', *Mechanism and Machine Theory*, Vol. 70, pp.298–319.

Chittenden, R.J., Dowson, D., Dunn, J.F. and Taylor, C.M. (1985) 'A theoretical analysis of the isothermal elastohydrodynamic lubrication of concentrated contacts: II: general case, with lubricant entrainment along either principal axis of the Hertzian contact ellipse or at some intermediate angle', *Proc. Roy. Soc., Ser. A*, Vol. 397, No. 1813, pp.271–294.

Dong, W., Xing, Y., Moan, T. and Gao, Z. (2013) 'Time domain-based gear contact fatigue analysis of a wind turbine drivetrain under dynamic conditions', *Int. J. Fatigue*, Vol. 48, pp.133–146.

Evans, C.R. and Johnson, K.L. (1986) 'Regimes of traction in elastohydrodynamic lubrication', *Proc. IMechE, Part C: J. Mechanical Engineering Science*, Vol. 200, No. 5, pp.313–324.

Fatourehchi, E., Elisaus, V., Mohammadpour, M., Theodossiades, S. and Rahnejat, H. (2016) 'Efficiency and durability predictions of high performance racing transmissions', *SAE Int., J. Passenger Cars-Mechanical Systems*, Vol. 9, 2016-01-1852.

Fatourehchi, E., Mohammadpour, M., King, P.D., Rahnejat, H., Trimmer, G. and Williams, A. (2018) 'Microgeometrical tooth profile modification influencing efficiency of planetary hub gears', *International Journal of Powertrains*, Vol. 7, Nos. 1–3, pp.162–79.

Fatourehchi, E., Mohammadpour, M., King, P.D., Rahnejat, H., Trimmer, G., Williams, A. and Womersley, R. (2017) 'Effect of mesh phasing on the transmission efficiency and dynamic performance of wheel hub planetary gear sets', *Proceedings of the Institution of Mechanical Engineers*, *Part C: Journal of Mechanical Engineering Science*, DOI: 0954406217737327.

Gohar, R. and Rahnejat, H. (2008) *Fundamentals of Tribology*, Imperial College Press, London.

Greenwood, J.A. and Tripp, J.H. (1970) 'The contact of two nominally flat rough surfaces', *Proc. IMechE*, Vol. 185, No. 3, pp.625–633.

Jao, T.C., Henly, T., Carlson, G.W., Ved, C., Carter, R.O., Hildebrand, D.H. and Ogorek, W. (2006) *Planetary Gear Fatigue Behavior in Automatic Transmission*, SAE Technical Paper.

Johnson, K.L. (1985) *Contact Mechanics*, Cambridge University Press, Cambridge, UK.

Johns-Rahnejat, P.M. (1988) *Pressure and Stress Distribution Under Elastohydrodynamic Point Contacts*, PhD thesis, Imperial College, London.

Johns-Rahnejat, P.M. and Gohar, R. (1997) 'Point contact elastohydrodynamic pressure distribution and sub-surface stress field', in *Tri-Annual Conference on Multi-Body Dynamics: Monitoring and Simulation Techniques*.

Karagiannis, I., Theodossiades, S. and Rahnejat, H. (2012) 'On the dynamics of lubricated hypoid gears', *Mechanism and Machine Theory*, Vol. 8, pp.94–120.

Li, S., Kahraman, A. and Klein, M. (2012) 'A fatigue model for spur gear contacts operating under mixed elastohydrodynamic lubrication conditions', *Trans. ASME, J. Mechanical Design*, Vol. 134, No. 4, p.41007.

Ligata, H., Kahraman, A. and Singh A. (2008) 'An experimental study of the influence of manufacturing errors on the planetary gear stresses and planet load sharing', *Journal of Mechanical Design*, 1 April, Vol. 130, No. 4, p.41701.

Lundberg, G. and Palmgren, A. (1949) 'Dynamic capacity of rolling bearings', *Trans. ASME, J. Applied Mechanics*, Vol. 16, No. 2, pp.165–72.

Marques, P.M., Camacho, R., Martins, R.C. and Seabra, J.H. (2015) 'Efficiency of a planetary multiplier gearbox: influence of operating conditions and gear oil formulation', *Tribology International*, Vol. 92, pp.272–280.

Mohammadpour, M., Theodossiades, S. and Rahnejat, H. (2014) 'Transient mixed non-Newtonian thermo-elastohydrodynamics of vehicle differential hypoid gears with starved partial counter-flow inlet boundary', *Proc. IMechE*, *Part J: J. Engineering Tribology*, Vol. 228, No. 10, pp.1159–1173.

Mohammadpour, M., Theodossiades, S. and Rahnejat, H. (2016) 'Dynamics and efficiency of planetary gear sets for hybrid powertrains', *Proc. IMechE, Part C: J. Mechanical Engineering Science*, Vol. 230, Nos. 7–8, pp.1359–1368.

Talbot, D.C., Kahraman, A. and Singh, A. (2012) 'An experimental investigation of the efficiency of planetary gear sets', *Trans. ASME, J. Mechanical Design*, Vol. 134, No. 2, p.21.

Teodorescu, M., Balakrishnan, S. and Rahnejat, H. (2005) 'Integrated tribological analysis within a multi-physics approach to system dynamics', *Tribology and Interface Engineering Series*, Vol. 48, pp.725–737.

Teodorescu, M., Kushwaha, M., Rahnejat, H. and Rothberg, S.J. (2007) 'Multi-physics analysis of valve train systems: from system level to microscale interactions', *Proc. IMechE, Part K: J. Multi-body Dynamics*, Vol. 221, No. 3, pp.349–361.

Vijayakar, S. (2000) *CALYX Manual*, Advanced Numerical Solutions Inc., Columbus, Ohio, USA.

Vijayakar, S.M. (1996) 'Edge effects in gear tooth contact', in *Proc. of the 7th International Power Transmission and Gearing Conference*, Vol. 88, pp.205–212.

Xu, H. and Kahraman, A. (2007) 'Prediction of friction-related power losses of hypoid gear pairs', *Proc. IMechE, Part K: J. Multi-Body Dynamics*, Vol. 221, No. 3, pp.387–400.

Nomenclature

A	Apparent contact area
$\boldsymbol{c}$□	Specific heat capacity of the solid surfaces
$\boldsymbol{E}_r$	Reduced elastic modulus of the contact
$\boldsymbol{E}$□	Reduced elastic modulus of the contact: $(2E_r) / \pi$
EHL	Elastohydrodynamic lubrication
fv	Viscous friction
$\boldsymbol{h}^*_{c0}$	Dimensionless central lubricant film thickness
$\boldsymbol{h}_{c0}$	Central lubricant film thickness
$\boldsymbol{K}$	Lubricant's thermal conductivity
$\boldsymbol{K}$□	Thermal conductivity of the solids
$\overline{\boldsymbol{p}}$	Average (Laplace) contact pressure
P_m	Mean pressure
q	Traction
R	Effective radii of curvature
R_x	Radii of curvature along the direction of sliding
R_y	Radii of curvature along the direction of side leakage
TCA	Tooth contact analysis
U_r	Rolling velocity
U_s	Sliding velocity
U	Speed of entraining motion
α	Pressure viscosity coefficient
β	Average asperity tip radius
η_0	Lubricant dynamic viscosity at atmospheric pressure
μ	Coefficient of friction
$\boldsymbol{\rho}'$	Density of solids
τ_0	Eyring shear stress